

Comparative study by simulation between two structures CdS/CZTS and ZnS/CZTS via SCAPS-1D software

C.E.H. Merzouk^a, S. Bensmaine^a, L. Ghalmi^a, A. Aissat^{b,c} *

^aURMERR Research Unit on Renewable Materials and Energies, Department of Physics, Abou Bakr Belkaid University Tlemcen, (UABT), BP n°119, Algeria

^bLATSI Laboratory, Department of electronics, Faculty of Technology, University of Saad Dahlab, Blida1, Blida 09000, Algeria

^cUniversity of Ahmed Draya, Adrar Algeria

This comparative numerical simulation study investigates the electrical characteristics of two heterojunction thin-film solar cells based on Kesterites Copper Zinc Tin Sulfide. The study compared two solar cells with different structures, Zinc Oxide ZnO/Cadmium Sulfide CdS/Kesterites CZTS/Molybdenum Mo and Zinc Oxide ZnO/Zinc Sulfide ZnS/Kesterites CZTS/Molybdenum Mo, to determine which is more efficient in achieving maximum photovoltaic efficiency. The results showed that the ZnO/ZnS/CZTS/Mo solar cell is the better option, outperforming the CdS/CZTS/Mo solar cell in terms of short-circuit current density J_{sc} , open-circuit voltage V_{oc} , form factor FF, and photovoltaic efficiency η . The study also investigated the effect of doping and layer thickness of CZTS and ZnS on photovoltaic parameters. The optimized ZnS/CZTS solar cell achieved an efficiency of 16.29% for ZnS and CZTS layer thicknesses of 0.02 μm and 4 μm , respectively, and doping concentrations of 10^{18} and 10^{16}cm^{-3} , respectively. Overall, this study provides valuable insights for designing more efficient solar cells and optimizing their photovoltaic efficiency using Kesterites CZTS, CdS, and ZnS materials.

(Received September 30, 2023; Accepted February 1, 2024)

Keywords: Kesterites CZTS, Buffer layer, Cadmium sulfide CdS, Zinc sulfide ZnS, Solar cells

1. Introduction

Heterojunction thin-film solar cells based on Kesterites Copper Zinc Tin Sulfide have emerged as a promising candidate for next-generation photovoltaic devices due to their low-cost, non-toxic, and earth-abundant constituents [1,2]. In this comparative numerical simulation study, we investigated the electrical characteristics of two heterojunction thin-film solar cells based on Kesterites. The performance of two solar cells was compared with different buffer layers using the Solar Cell Capacitance Simulator SCAPS-1D software.

One of the solar cells was fabricated with a Cadmium Sulfide CdS buffer layer, while the other cell was fabricated with a Zinc Sulfide ZnS buffer layer. The two cells had the same structure: Zinc Oxide ZnO/buffer layer/CZTS/Molybdenum Mo. The effect of doping the buffer/absorber layer and its thickness on the photovoltaic parameters such as short circuit current density J_{sc} , open-circuit voltage V_{oc} , form factor FF, and photovoltaic efficiency η was investigated in detail.

The results showed that the ZnO/ZnS/CZTS/Mo solar cell outperformed the CdS/CZTS/Mo solar cell in terms of J_{sc} , V_{oc} , FF, and η . The simulations also revealed that the effect of doping the buffer/absorber layer and its thickness on photovoltaic parameters was significant. Increasing the thickness of the buffer/absorber layer led to an increase in J_{sc} but a decrease in V_{oc} . However, J_{sc} reached a plateau beyond a certain thickness. Similarly, increasing the doping of the buffer/absorber layer resulted in an increase in J_{sc} but a decrease in V_{oc} .

* Corresponding author: sakre23@yahoo.fr
<https://doi.org/10.15251/CL.2024.212.113>

Several previous studies have reported the fabrication and characterization of CZTS-based solar cells. For example, G. K. Dalapati *et al* reported the fabrication of CZTS solar cells with a power conversion efficiency η of 4.2% using a CdS buffer layer [3].

Similarly, M. F. Islam *et al* reported the fabrication of CZTS solar cells with a η of 5.2% using a ZnS buffer layer [4]. In contrast, our study focused on the electrical characterization of CZTS-based solar cells with different buffer layers using numerical simulations.

In recent years, numerical simulations have emerged as a powerful tool for the design and optimization of photovoltaic devices [5]. Several studies have reported the use of numerical simulations to investigate the electrical characteristics of CZTS-based solar cells. For example, F. A. Jhuma *et al* employed numerical simulations to study the impact of the buffer layer thickness on CZTS solar cell performance [6]. In a separate study, F. A. Jhuma and M. J. Rashid also utilized numerical simulations to optimize the doping concentration of the CdS buffer layer for CZTS solar cells [7].

The objective of this comparative numerical simulation study was to investigate the electrical characteristics of two heterojunction thin film solar cells based on K esterites CZTS with different buffer layers, CdS and ZnS. The aim was to determine which of the two solar cells would achieve maximum photovoltaic efficiency by analyzing the photovoltaic parameters such as J_{sc} , V_{oc} , FF, and η while varying the thickness and doping of the buffer/absorber layer.

The novelty of this work lies in the comparison of the performance of CZTS-based solar cells with two different buffer layers using numerical simulations. Additionally, the study highlights the significance of the thickness and doping of the buffer/absorber layer on the photovoltaic parameters, which can aid in the optimization and design of CZTS-based solar cells with better efficiency.

2. Theoretical model

In its most common configuration, a CZTS cell consists of a stack of several thin film materials deposited continuously on a substrate. The substrate is usually a soda lime glass SLG plate. Figure 1 shows the standard structure of a CZTS cell [8].

CZTS solar cells contain absorbers composed of copper, zinc, tin, and sulfur. This 1-2.5 μm thick layer is p-doped and needs to be coated with an n-type material constituting the first part of the p-n heterojunction, such as cadmium sulfide CdS. However, due to the toxicity of cadmium, research has turned to the development of alternative buffer layers Zn (O, S), Zn, Mg O, etc. The thickness of the buffer layer varies from 0.04 to 0.07 μm and is covered by a window layer which consists of zinc oxide ZnO deposits. Therefore, the ZnO layer is resistive and serves to limit the form of short circuit in the imperfect area of the CZTS covered by the buffer layer [9]. The most widely used TCO Transparent Conductive Oxides is aluminum doped ZnO:Al, indium oxide In_2O_3 and tin SnO_2 sputter deposited. The thickness of the optical window layer is between 300 nm and 500 nm. The final front contact consists of a Nickel and Aluminum based grid to collect the charge generated by the device.

$\text{Cu}_2\text{ZnSnS}_4$ is a $\text{I}_2\text{-II-IV-VI}_4$ semiconductor. Experimentally, $\text{Cu}_2\text{ZnSnS}_4$ usually crystallizes with a K esterites structure [10-11-12] or a stannite structure. In both cases it is a central quadratic grid. Chalcopyrite is considered the most stable battery [13]. Its mesh parameters are $a=0.54$ nm and $c=1.09$ nm [14]. It is generally expressed as a structure derived from the chalcopyrite structure, in which the In^{3+} ions are replaced by Zn^{2+} and Sn^{4+} ions. The stannite structure differs from K esterites only in the positioning of Cu^+ and Zn^{2+} [15].

We have noticed from several works that the best current buffer layer is cadmium sulfide (chalcogenide). Indeed, the combination of the buffer layer and the zinc oxide window layer makes it possible to establish performance records based on the CZTS technology. However, given the toxicity of the element cadmium, its use is controversial. Other candidate layers such as In_2S_3 have been proven, but unfortunately the cell is still affected by the cost of the extra indium.

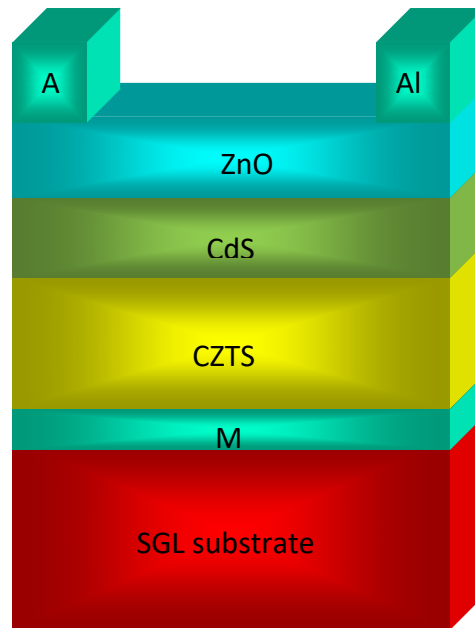


Fig. 1. Basic structure of CZTS solar cell [8].

Therefore, current research is turning to quilted layers that do not present such obstacles. For this reason, zinc chalcogenide based thin films are very interesting candidates. Although the performance of solar cells using CZTS/CdS PN junctions is very good, the bandgap energy of cadmium sulfide is quite low, about 2.4 eV, which presents absorption defects. Indeed, through the transparent electrode, the window layer and the buffer layer, the transmittance of the incident light must be maximized and as wide as possible in the electromagnetic spectrum [16].

Therefore, specifications for zinc chalcogenide buffer layers include: A bandgap energy large enough not to degrade battery performance; A bandgap energy tunability to achieve conduction band positioning between the conduction band of the CZTS and the conduction band of the ZnO window layer and can also minimize the proportion of copper in the CZTS layer; A suitable charge density $N(\text{cm}^{-3})$ to limit the recombination phenomenon N-type semiconductor; A quality of the interface with the layer CZTS used to control the diffusion of defects at the interface.

With bandgap energies of about 3.3 and 3.7 eV, respectively, zinc oxide ZnO and zinc sulfide (ZnS) are a priori very suitable materials for such applications [17]. Given our interest in the effect of temperature on the improvement of solar cell performance [18], it would be interesting to introduce the concept of coefficient of thermal expansion which has an impact on the durability of thin film solar cells [19]. When exposed to temperature variations, the layers of the cell expand or contract at different rates, creating internal stresses that can affect performance and durability. Solar cell manufacturers use materials with similar coefficients of thermal expansion, add intermediate layers, and use special layer deposition techniques to minimize these effects [19]. Thus, the coefficient of thermal expansion is an important factor in the design and manufacture of thin-film solar cells to ensure their long-term reliability and performance [20].

3. Results and discussion

We introduce the concept of numerical simulation of semiconductors, especially the application on solar cells of the type CZTS using the SCAPS-1D calculation software. The values we used for the calculation with SCAPS software are taken from the literature [21] and are shown in Table1 for the cell CZTS/ (CdS/ ZnS) /ZnO/ZnO: Al. The absorption coefficients of (CZTS), (CdS), (ZnS), ZnO:Al and ZnO-i are taken from SCAPS-1D. We propose to simulate the essential

properties of a CZTS-based cell with a structure composed of a transparent conductive oxide TCO of the n-ZnO type, a buffer layer of the n-CdS or n-ZnS type and an absorbing layer of the p-CZTS type Figure2.

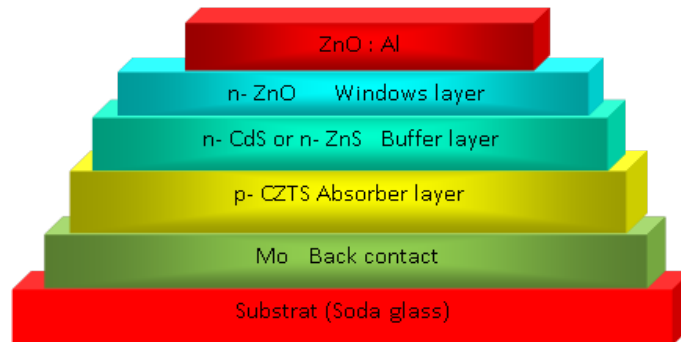


Fig.2. Structure of the CZTS solar cell The ZnO/(CdS(n) or ZnS(n))/CZTS(p)/Mo cell.

Table. 1 Parameters of the materials used in this design.

Settings	Absorber, p-CZTS	Buffer layer, n-CdS	Buffer layer, n-ZnS	Window layer ZnO	ZnO: Al
Thickness (nm)	500	20	20	50	200
Gap energy (eV)	1.5	2.45	3.68	3.3	3.3
Affinity (eV)	4.58	4.2	4.5	4.55	4.55
dielectric permittivity (relative)	9.5	8.9	8.32	8	8
State densities in BC, $N_c(\text{cm}^{-3})$	1.91×10^{18}	2.52×10^{18}	1.5×10^{18}	4.1×10^{18}	4.1×10^{18}
State densities in BV $N_v(\text{cm}^{-3})$	2.58×10^{18}	2.01×10^{18}	1.8×10^{19}	8.20×10^{18}	8.20×10^{18}
Electron speed $V_e(\text{cm/s})$	2.750×10^7	2.12×10^7	1.0×10^7	1.73×10^7	1.73×10^7
Hole speed, $V_{\text{hole}}(\text{cm/s})$	2.120×10^7	1.18×10^7	1.0×10^{17}	1.03×10^7	1.03×10^7
Electron mobility $\mu_n(\text{cm}^2/\text{V.s})$	50	50	250	100	100
Hole mobility $\mu_p(\text{cm}^2/\text{V.s})$	10	20	40	20	20
Defect density $N_D(\text{donor})(\text{cm}^{-3})$	0	1×10^{18}	1.0×10^{18}	1×10^{10}	1.0×10^{20}
Defect Density Acceptor $N_A(\text{cm}^{-3})$	1.0×10^{16}	0	0	0	0
WG (eV)	0.1	0.1	0.1	0.1	0.1
Electron Capture Section (cm^2)	5×10^{-17}	10^{-17}	10^{-17}	10^{-12}	10^{-12}
Hole Capture Section (cm^2)	10^{-13}	10^{-12}	10^{-12}	10^{-15}	10^{-15}

Solar cells based on cadmium sulfide CdS and copper zinc tin sulfide CZTS have shown promising performance in converting solar energy into electricity. However, the toxicity of cadmium is a major environmental and health concern. In this study, we replaced the CdS buffer layer with zinc sulfide ZnS due to its non-toxicity and abundance in nature.

Table. 2 Comparison of the important parameters in the CdS and ZnS cells.

Simulated solar cell	$J_{\text{sc}}(\text{mA}/\text{cm}^2)$	$V_{\text{oc}}(\text{V})$	FF (%)	η (%)
CZTS/ZnS/ZnO	28.06	0.64	83.53 %	15.04
CZTS/CdS/ZnO	28.72	0.65	82.95	15.46

We simulated solar cells with different buffer layers and obtained the following parameters under AM 1.5 solar spectrum with power density 1000 W/m^2 : open circuit voltage V_{oc} of 0.65 V, short circuit current density (J_{sc}) of $28.72 \text{ mA}/\text{cm}^2$, form factor FF of 82.95% and

conversion efficiency (η) of 15.46% for the CdS/CZTS solar cell; and J_{sc} of 28.06 mA/cm², V_{oc} of 641.80 mV, FF of 83.53 % and η of 15.04% for the ZnS/CZTS solar cell. Table 2 and Figure 3 represents the J(V) characteristics of the two structures studied.

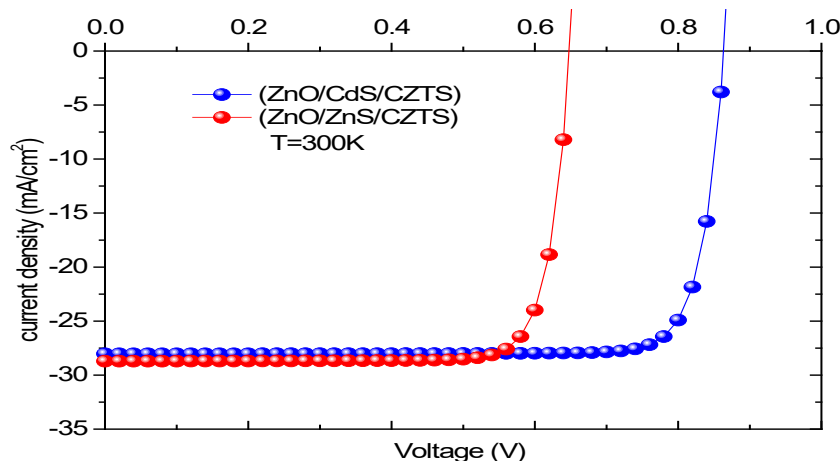


Fig. 3. J-V curves of CdS/CZTS and ZnS/CZTS solar cells.

Our results indicate that the ZnS/CZTS solar cell performs similarly to the CdS/CZTS solar cell in terms of J_{sc} , V_{oc} , FF and η . The higher band gap of ZnS compared to CdS allows for the transmission of higher energy photons, which could potentially improve the efficiency of the solar cell. Our next step is to study the effect of doping and thickness of the ZnS and CZTS layers to further optimize the solar cell parameters.

3.1. Effect of doping concentration on the CZTS layer

For a layer of ZnS 0.02 μ m and CZTS 0.5 μ m, we calculated the solar cell parameters for different values of the doping concentration N_d of CZTS between 1×10^{13} cm⁻³ and 1×10^{16} cm⁻³. The findings from Figures 4 and 5 demonstrate that the electrical parameters of the ZnS/CZTS solar cell are affected by the doping concentration. Specifically, as the doping concentration increases, there is a decrease in the short-circuit current density J_{sc} , which is attributed to an increase in recombination centers.

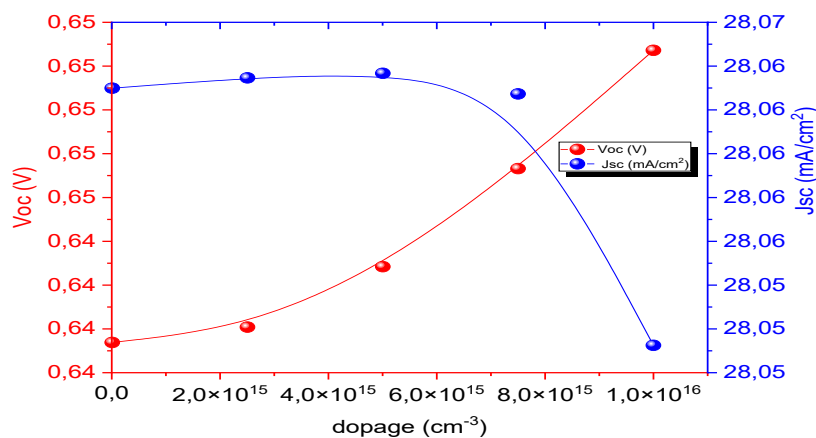


Fig.4. Open-circuit voltage and short-circuit current density as a function of doping Concentration in CZTS of the solar cell.

However, the open circuit voltage V_{oc} increases, potentially due to a reduction in the forbidden band and an increase in the integrated potential, contributing to an improvement in efficiency Figure 5 conversely, an increase in defect density caused by the higher doping concentration results in a decrease in the fill factor FF of the ZnS/CZTS solar cell. Nevertheless, adjusting the doping concentration carefully can lead to an overall improvement in efficiency Figure 6 These findings highlight the complex interplay between doping concentration and various electrical parameters of the ZnS/CZTS solar cell.

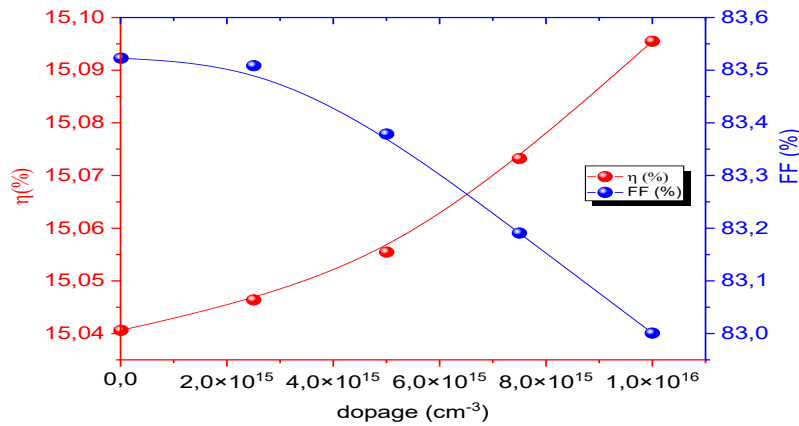


Fig.5. Efficiency and Fill Factor as a function of doping concentration in CZTS of the solar cell.

3.2. Effect of CZTS layer thickness

The thickness of the CZTS layer varies from 0.5 μm to 4 μm . The effect of the CZTS layer thickness on the solar cell is shown in Figure 6 and 7.

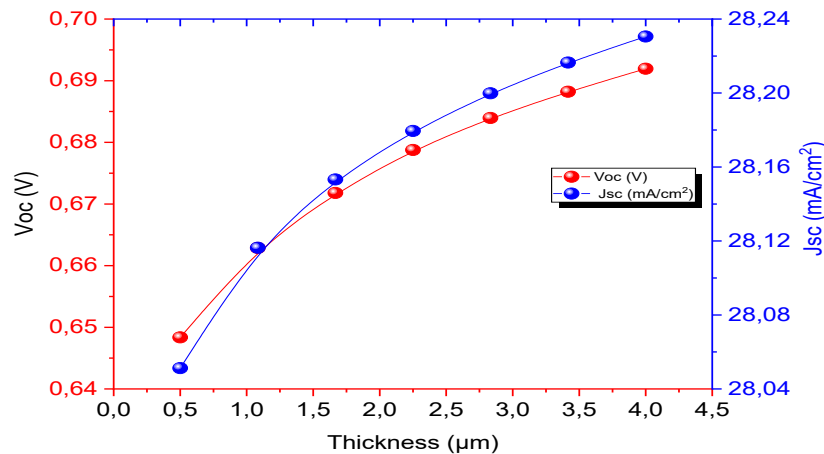


Fig. 6. Open-circuit voltage and short-circuit current density as a function of the CZTS layer thickness.

The thickness of the CZTS layer can have a significant impact on the electrical parameters of CZTS solar cells. Specifically, the J_{sc} tends to increase with increasing thickness, which can be attributed to higher absorption of incident light. In addition, the V_{oc} also tends to increase with increasing thickness, indicating a reduction in recombination losses within the bulk of the CZTS layer Figure 6. However, the fill factor FF tends to decrease with increasing thickness, which may

be due to an increase in defect density and recombination losses. Despite this, the power conversion efficiency η generally increases with increasing thickness, likely due to a trade-off between the increase in J_{sc} and the decrease in FF (Figure 7).

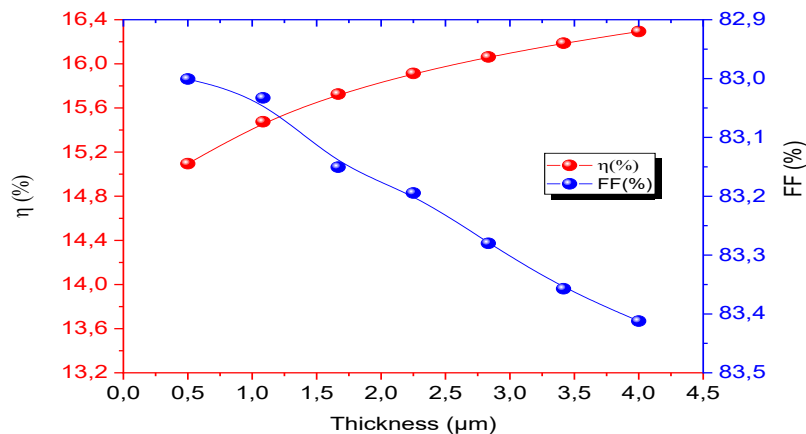


Fig. 7. Efficiency and Fill Factor as a function of the CZTS layer thickness.

It is worth noting that the optimal thickness of the CZTS layer depends on various factors, such as the type of materials used and the processing conditions. Therefore, careful optimization of the CZTS layer thickness is crucial to achieving high performance in CZTS solar cells.

3.3. Effect of ZnS layer thickness

The thickness of the ZnS layer varies from 0.02 μm to 0.05 μm . The effect of ZnS layer thickness on the solar cell is shown in Figures 8 and 9. The buffer layer in a solar cell makes it possible to improve the efficiency of the device by reducing the recombination of charge carriers at the interface between the absorbing layer and the transport layer. In the case of a ZnS buffer layer, its thickness can significantly affect the electrical parameters of the solar cell. We notice that a thinner ZnS layer can lead to a higher V_{oc} because it reduces the height of the barrier for electron transport from the absorber layer to the transport layer. The thickness of the ZnS layer can also affect light absorption in the solar cell. A thicker ZnS layer may cause a decrease in J_{sc} due to increased reflection and absorption losses Figure 8.

When the ZnS buffer layer is thick enough, it acts as a surface passivation layer to reduce surface defects and minimize charge carrier recombination at interfaces between layers. This reduces series resistance and improves charge collection, which leads to an increase in the FF of our ZnS/CZTS solar cell. We observe that a moderate thickness of the ZnS layer lead to the highest η , which is the ultimate goal of improving the efficiency of the solar cell. Therefore, optimizing the thickness of the ZnS buffer layer is crucial for achieving the highest possible efficiency of the ZnS/CZTS solar cell Figure 9. Our optimization process has shown that the most effective doping for the (ZnS) layer is $1 \times 10^{18} \text{ cm}^{-3}$ with a thin thickness of 0.020 μm , while the ideal doping for the (CZTS) layer is $1 \times 10^{16} \text{ cm}^{-3}$ with a thin thickness of 4 μm . These optimized parameters have resulted in an impressive electrical efficiency of 16.29% in CZTS solar cells. These findings corroborate previous studies that have also explored the use of ZnS as an alternative to CdS in CZTS solar cells Table 3.

For instance, K. Sunand et al reported on the effect of employing Zn_{0.35}Cd_{0.65}S as the novel buffer material on the performance of CZTS solar cells and achieved a power conversion efficiency of 9.2% [22]. B. Yassine *et al* achieved a conversion efficiency of 14.61% using a ZnS buffer layer in CZTS solar cells [23]. Also, Boubakeur *et al* found an efficiency of 14.59% [24]. Our work demonstrates that ZnS is an effective and sustainable buffer layer material that can replace CdS without sacrificing performance. This is a significant step towards developing environmentally friendly and non-toxic solar cell technologies

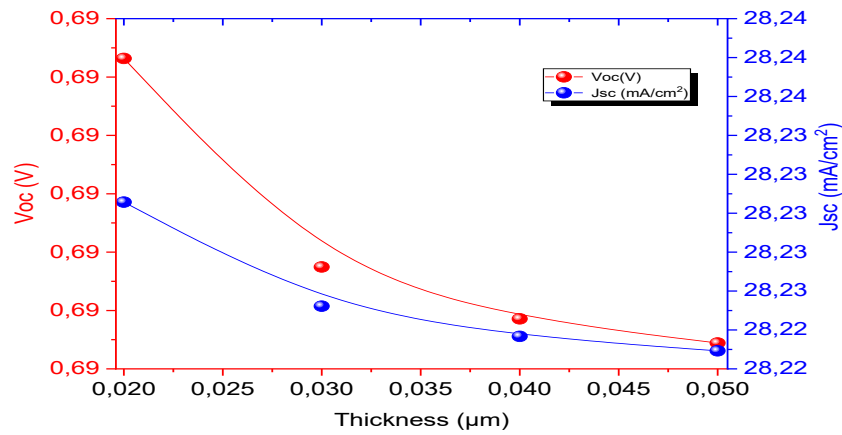


Fig. 8. Open-circuit voltage and short-circuit current density as a function of the ZnS layer thickness.

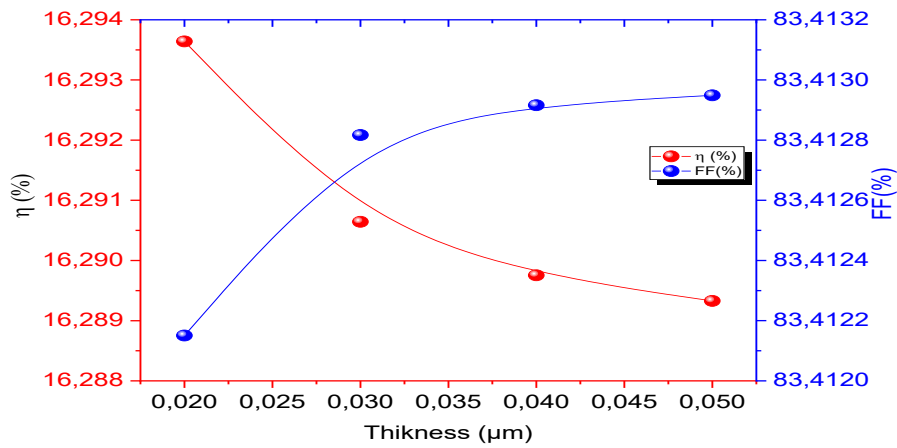


Fig. 9. Efficiency and Fill Factor as a function of the ZnS layer thickness.

Table. 3 Optimal parameters of CZTS solar cell.

ZnS		CZTS		η (%)	FF (%)	V _{oc} (mV)	J _{sc} (mA/cm ²)
thickness (nm)	N _d (cm ⁻³)	thickness (μm)	N _d (cm ⁻³)				
20	1x10 ¹⁸	4	1x10 ¹⁶	16.29	83.41	700	28.41

3.4. Influence of temperature on the parameters of the CZTS optimal cell

The operating temperature of CZTS solar cells has a significant impact on their performance. We have found that as the temperature increases, the bandgap energy of CZTS decreases, which affects the cell's ability to absorb photons and generate charge carriers. Figure 10 shows the variation of the bandgap energy of CZTS for different temperatures ranging from 300K to 400K.

Furthermore, we have observed a linear decrease in the open circuit voltage (V_{oc}) of the ZnS/CZTS cell with increasing temperature, as depicted in Figure 11 at 300K, the value of V_{oc} is 0.691V, while at 400K, it drops to 0.67V. This decrease in V_{oc} is due to the increase in the density of states of CZTS at higher temperatures. Additionally, we have observed a decrease in the fill

factor FF of the ZnS/CZTS cell with increasing temperature, as shown in Figure 12. This is caused by the decrease in V_{oc} and the increase in the short circuit current J_{sc} Table.4.

Table 4. J - V parameters for different temperature values T .

T (K)	V_{oc} (V)	J_{sc} (mA/cm ²)	FF(%)	η (%)
300	0.70	28,23	83,41	16,29
310	0,69	28,24	82,97	16,18
320	0,69	28,27	82,54	16,04
330	0,68	28,29	82,094	15,92
340	0,68	28,35	81,67	15,82
350	0,68	28,40	81,23	15,73

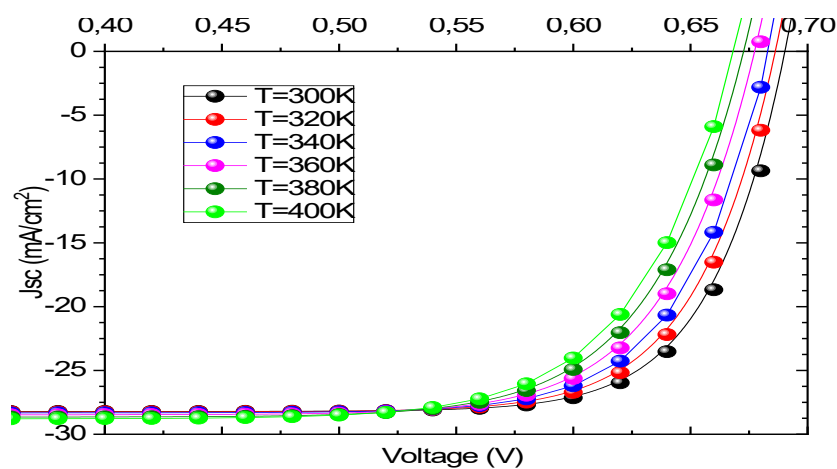


Fig. 10. $J(V)$ Characteristic of the solar cell for different temperature values.

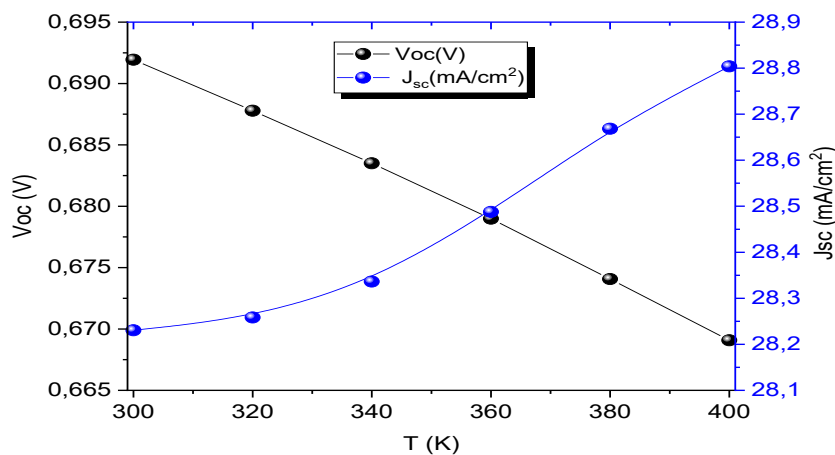


Fig. 11. Open-circuit voltage and short-circuit current density as a function of the temperature.

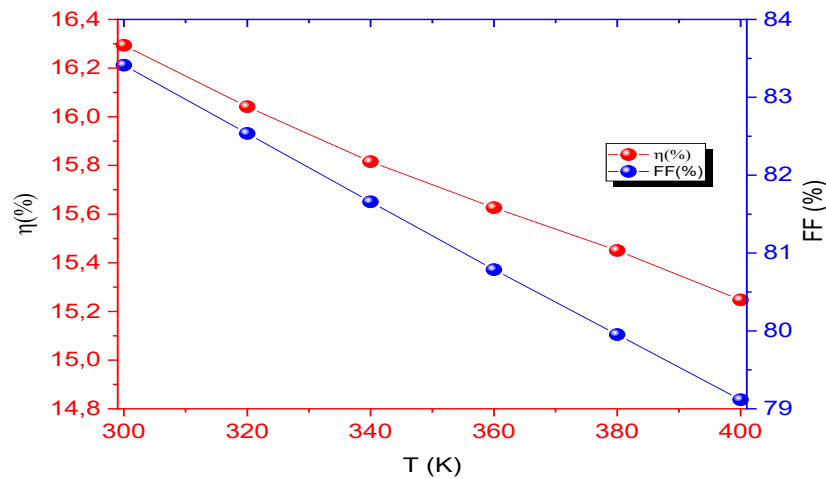


Fig. 12. Efficiency and Fill Factor as a function of the temperature.

Finally, we have found that the conversion efficiency of the ZnS/CZTS cell decreases with increasing temperature due to the combined effect of the decrease in V_{oc} and FF, as shown in Figure 11. Overall, our results demonstrate the importance of carefully controlling the operating temperature of CZTS solar cells to achieve optimal performance.

While simulations provide a valuable tool for studying solar cell behavior, it is crucial to validate the results with experimental data. The variations observed between simulation and experimental results highlight the complex nature of solar cell performance and the need for further research to improve the accuracy of simulations. Additional experiments, detailed characterization, and parameter optimization can help bridge the band gap energy between simulations and real world performance, leading to better understanding and design of efficient solar cells (Table 5).

The validation of our simulation results with other simulation [25,26] and experimental [27] results have been presented. For the first structure Mo/CZTS/CdS/ZnO/ZnO:Al we obtained an efficiency of 15.46%. We had a relative gain in efficiency compared to the result of ref [25] of 9%. However, the second structure Mo/CZTS/ZnS/ZnO/ZnO:Al presents a relative benefit of 19.6% compared to the result of ref [26]. In addition, the best results, that are obtained with the second structure, were compared with the experimental results ref [27], and a relative gain of 46% have been reached. Finally, this study allows us to produce a solar cell with an efficiency of 16.29% with a less toxic structure.

Table. 5 Comparison of the important parameters in the proposed design and the published designs.

Solar Cells	J_{sc} (mA/cm ²)	V_{oc} (V)	FF (%)	η (%)
Mo/CZTS/CdS/ZnO/ZnO :Al Simulated	28.72	0.65	82.95	15.46
Mo/CZTS/CdS/ZnO/ZnO :Al Simulation [25]	35.06	0.75	53.13	14.06
Mo/CZTS/ZnS/ZnO/ZnO :Al Simulated	28.41	0.70	83.41	16.29
Mo/CZTS/ZnS/ZnO/ZnO :Al Simulation [26]	20.20	0.96	67.30	13.10
Mo/CZTS/ZnS/ZnO/ZnO :Al Experimental [27]	20.70	0.68	62.50	08.80

4. Conclusion

Simulation of two solar cells with structures: ZnO/CdS(n)/CZTS(p) and ZnO/ZnS(n)/CZTS(p) using the SCAPC software shows that the solar cell with the ZnS buffer layer gives an efficiency $\eta=15.04\%$ while the one designed with the CdS buffer layer gives an efficiency $\eta=15.49\%$. The yields are almost the same and to avoid the toxicity of the cadmium Cd substance

contained in the cadmium sulfide CdS, we found that zinc sulfide ZnS material is more suitable to replace cadmium sulfide CdS and the short wavelength light absorption rate of CdS material is higher than that of ZnS material $E_g(\text{ZnS}) > E_g(\text{CdS})$. We optimized the ZnS/CZTS solar cell by investigating the effect of doping and layer thickness of CZTS and ZnS. The optimal efficiency obtained is 16.29% for ZnS and CZTS layer thicknesses of the order of $0.02\mu\text{m}$ and $4\mu\text{m}$ respectively and doped with concentrations of the order of 10^{18}cm^{-3} and 10^{16}cm^{-3} respectively.

References

- [1] W. Wang, M. T. Winkler, O. Gunawan, T. Gokmen, T. K. Todorov, Y. Zhu, D. B. Mitzi, *Adv. Energy Mater.*, 4(7), 1301465(2014); <https://doi.org/10.1002/aenm.201301465>
- [2] L. Ghalmi, S. Bensmaïne, M. Elbar, S. Chala, H. Merzouk, *J. Nano- Electron. Phys.* 14(6), 06033 (2022); [https://doi.org/10.21272/jnep.14\(6\).06033](https://doi.org/10.21272/jnep.14(6).06033)
- [3] G. K. Dalapati, S. Zhuk, S. Masudy-Panah, A. Kushwaha, H. L. Seng, V. Chellappan, S. Tripathy, *Scientific reports*, 7(1), 1350(2017); <https://doi.org/10.1038/s41598-017-01605-7>
- [4] M. F. Islam, N. M. Yatim, M. A. Hashim, *Journal of Advanced Research in Fluid Mechanics and Thermal Sciences*, 81(1), 73-87(2021); <https://doi.org/10.37934/arfmts.81.1.7387>
- [5] A. Haddout, A. Raidou, M. Fahoume, *Applied Physics A*, 125, 1-16.124(2019); <https://doi.org/10.1007/s00339-019-2413-3>
- [6] F. A. Jhuma, M. Z. Shaily, M. J. Rashid, *Materials for Renewable and Sustainable Energy*, 8, 1-7(2019); <https://doi.org/10.1007/s40243-019-0144-1>
- [7] F. A. Jhuma, M. J. Rashid, *Journal of theoretical and applied physics*, 14, 75-84(2020); <https://doi.org/10.1007/s40094-019-00363-3>
- [8] S. Enayati Maklavani, S. Mohammadnejad, *Optical and Quantum Electronics*, 52, 1-22(2020); <https://doi.org/10.1007/s11082-019-2180-6>
- [9] U. Rau, P. O. Grabitz, J. H. Werner, *Applied Physics Letters*, 85(24), 6010-6012(2004); <https://doi.org/10.1063/1.1835536>
- [10] S. Guitouni, PhD thesis, University OF Mentouri-Constantine1, (2017); <http://depot.umc.edu.dz/handle/123456789/9513>
- [11] X. Lin, J. Kavalakkatt, K. Kornhuber, S. Levchenko, M. C. Lux-Steiner, A. Ennaoui, *Thin Solid Films*, 535, 10-13(2013); <https://doi.org/10.1016/j.tsf.2012.10.034>
- [12] L. Elizabeth, Doctoral dissertation, The University of Utah. (2014).
- [13] T. Maeda, S. Nakamura, T. Wada, *MRS Online Proceedings Library (OPL)*, 1165, 1165-M04(2009); <https://doi.org/10.1557/proc-1165-m04-03>
- [14] S. R. Hall, J. T. Szymanski, J. M. Stewart, *Canadian Mineralogist*, 16(2), 131-137(1978).
- [15] M. D. Regulacio, C. Ye, S. H. Lim, M. Bosman, E. Ye, S. Chen, Q. H. Xu, M. Y. Han, *Chem. Eur. J.*, 18(11), 3127-3131(2012); <https://doi.org/10.1002/chem.201103635>
- [16] N. Naghavi, D. Aou-Ras, N. Allsop, N. Barreau, S. Bücheler, A. Ennaoui, C. H. Fischer, C. Guillen, D. Hariskos, J. Herrero, R. Klenk, K. Kushiya, D. Lincot, R. Menner, T. Nakada, C. Platzer-Björkman, S. Spiering, A. N. Tiwari, T. Törndahl, *Prog. Photovol: Res. Appl.*, 18411-433(2010); <https://doi.org/10.1002/pip.955>
- [17] J. Zagorac, D. Zagorac, V. Šrot, M. Randelović, M. Pejić, P. A. van Aken, J. C. Schön, *Materials*, 16(1), 326(2022); <https://doi.org/10.3390/ma16010326>
- [18] M. A. Green, K. Emery, Y. Hishikawa, W. Warta, E. D. Dunlop, *Solar cell efficiency tables, version 46, Progress in Photovoltaics: Research and Applications*, vol. 29, pp. 3 15(2021); <https://doi.org/10.1016/j.rser.2021.110782>
- [19] K. Mertens, *Photovoltaics: fundamentals, technology, and practice*, John Wiley & Sons, (2018).
- [20] M. M. de Lima Jr, R. G. Lacerda, J. Vilcarromero, F. C. Marques, *Journal of Applied Physics*, 86(9), 4936-4942(1999). <https://doi.org/10.1063/1.371463>
- [21] A. Srivastava, P. Dua, T. R. Lenka, & S. K. Tripathy, *Materials Today: Proceedings*, vol. 43, p. 3735-3739(2021); <https://doi.org/10.1016/j.matpr.2020.10.986>
- [22] K. Sun, C. Yan, F. Liu, J. Huang, F. Zhou, J. A. Stride, M. Green, *Adv Energy, Mater.*; 6(12):1600046 (2016); <https://doi.org/10.1002/aenm.201600046>

- [23] B. Yassine, B. Tahar, G. Fathi, Chalcogenide Letters Vol. 19(8) . 503 – 511(2022); <https://doi.org/10.15251/CL.2022.198.503>
- [24] M. Boubakeur, A. Aissat, L. Chenini, M. Ben Arbia, H. Maaref, J. P. Vilcot, Journal of Electronic Materials, 10-25 (2022); <https://DOI:10.1007/s11664-022-09986-w>
- [25] S. Kerour, A. Bouloufa, M. Lasladj, K. Djessas, K. Medjnoun, Journal of Semiconductors, 42(7), 072701(2021); <https://doi.org/10.1088/1674-4926/42/7/072701>
- [26] A.R. Latrous, R. Mahamdi, N. Touafek, M. Pasquinelli, Annales de Chimie - Science des Matériaux, 45(6), 431-437(2021); <https://doi.org/10.18280/acsm.450601>
- [27] C. Yan, K. Sun, J. Huang, S. Johnston, F. Liu, B.P. Veetil, X. Hao, ACS Energy Letters, 2(4), 930-936(2017); <https://doi.org/10.1021/acseenergylett.7b00129>